Journal of Molecular Catalysis A: Chemical 314 (2009) 102–109

Contents lists available at ScienceDirect

Journal of Molecular Catalysis A: Chemical

journal homepage: www.elsevier.com/locate/molcata

Experimental and theoretical characterization of NO_x species on Ag/α-Al_2O_3

Hanna Härelind Ingelsten[a,b,*], Anders Hellman[a,c], Hannes Kannisto[a,b], Henrik Grönbeck[a,c]

[a] Competence Centre for Catalysis, Chalmers University of Technology, SE-412 96 Göteborg, Sweden
[b] Applied Surface Chemistry, Department of Chemical and Biological Engineering, Chalmers University of Technology, SE-412 96 Göteborg, Sweden
[c] Department of Applied Physics, Chalmers University of Technology, SE-412 96 Göteborg, Sweden

ARTICLE INFO

Article history:
Received 15 May 2009
Received in revised form 26 August 2009
Accepted 28 August 2009
Available online 6 September 2009

Keywords:
Ag/Al_2O_3
NO_x surface species
DRIFT
DFT

ABSTRACT

The adsorption of NO_x species on α-alumina and Ag/α-alumina is investigated by *in situ* diffuse reflection infrared Fourier transform (DRIFT) spectroscopy and density functional theory (DFT) calculations. The vibrational spectra obtained by DRIFTS experiments show broad spectral bands in the range between 1650 and 1200 cm^{-1}. The absence of distinct features is attributed to the heterogeneity of powder samples, i.e., variation in Ag cluster size and α-alumina surface termination. DFT calculations are employed to evaluate ground-state structures and vibrational wavenumbers of different NO_x species adsorbed either on alumina or Ag_1–Ag_4 clusters supported on alumina. In agreement with experiments, Ag cluster size and surface termination strongly influence the calculated vibrational properties. Although, an unambiguous identification of surface species from the DRIFT spectra is difficult, the theoretical results provide valuable guidance. As such, this approach has the potential to further increase the understanding of the reaction mechanism during hydrocarbon assisted selective catalytic reduction (HC-SCR) of NO_x.

1. Introduction

The demand for decreased CO_2 emissions in combination with stringent NO_x regulations, call for alternative automotive regulations after-treatment systems. Combustion in oxygen excess, as in diesel- and lean-burn engines, significantly improves the fuel efficiency and thereby effectively reduces the CO_2 emissions. However, the oxygen rich exhaust gas obstructs the NO_x reduction ability of the generally used three-way catalyst (TWC). One promising technique to reduce NO_x in oxygen excess is hydrocarbon assisted selective catalytic reduction (HC-SCR). In particular, Ag supported on alumina has shown high activity for this reaction, see *e.g.* [1,2]. The Ag/Al_2O_3 system has been extensively studied in the scientific literature and it has, for instance, been shown that the active sites consist of very small silver clusters, Ag_n with $n < 8$ [2]. Although numerous experimental studies have clarified issues concerning this system, the state and structure of the Ag clusters remains elusive; metallic silver, silver oxides and silver aluminate phases have all been suggested [1,2].

In order to improve the performance of a catalyst, fundamental knowledge as to the nature of its catalytic activity is desirable. Spectroscopic methods, like IR spectroscopy, have traditionally been one of few experimental techniques able to follow the formation of intermediate species and reaction products on catalytic surfaces. Assignments of spectral features are, however, in most cases not straight forward. One example is NO_x chemistry on metal oxides, which include several different surface species, resulting in many, often overlapping, bands within a narrow wavenumber interval [3]. Assignments are often based on common knowledge derived from IR spectra obtained for NO_x on other metal oxides and may, therefore, not be applicable in the specific case. First-principles calculations of vibrational properties are one possible approach to this problem. This method has been used to characterize the vibrational properties of nitrite- and nitrate-surface species adsorbed on barium oxide (BaO) [4–6]. However, it should be realized that the validity of first-principles results are restricted by the choice of model catalyst. Hence, an inter-play between theory and experiment is often necessary.

In the present work, *in situ* diffuse reflection infrared Fourier transform (DRIFT) spectroscopy is used to monitor NO and NO_2 adsorption and the evolution of NO_x surface species on α-alumina and Ag/α-alumina powder samples. The evaluation of IR spectra is discussed in relation to results from first-principles calculations based on the density functional theory (DFT). The model catalyst in this work (experimental and theoretical) is α-alumina as this is an alumina phase with a well-defined structure. The stable surface of this phase is (0 0 0 1) [7,8]. Experiment and theory agrees that this facet is Al-terminated under ultra-high vacuum conditions, although other terminations can be present under ambient conditions [9]. To account for the various possibilities, three different

* Corresponding author at: Applied Surface Chemistry, Department of Chemical and Biological Engineering, Chalmers University of Technology, SE-412 96 Göteborg, Sweden. Tel.: +46 0 31 7722959; fax: +46 0 31 160062.
E-mail address: hannahi@chalmers.se (H.H. Ingelsten).

1381-1169/$ – see front matter © 2009 Elsevier B.V. All rights reserved.
doi:10.1016/j.molcata.2009.08.022

surface terminations will be considered and vibrational properties of NO_x surface species on α-alumina with and without silver are calculated.

2. Theoretical methods

The first-principles study was performed using the DFT as implemented in DACAPO [10,11]. The Kohn–Sham wavefunctions were expanded using plane-waves with a kinetic energy cutoff of 25 Ry, whereas a 50 Ry cutoff was used for the charge density grid. Ultra-soft pseudo-potentials [12] were used to describe the interaction between the valence electrons and the ionic cores. The exchange-correlation was treated within the generalized-gradient approximation (GGA) level, by the use of the spin-polarized parameterization according to Perdew, Burke and Ernzerhof (PBE) [13]. The (charged) nitrite and nitrate are calculated using a positive jellium background. The structure relaxations were performed within the quasi-Newton method, using the Hellmann–Feynman theorem for the force calculations. The ionic positions were optimized until the total residual force was less than 0.05 eV/Å.

The vibrational modes and energies were determined by diagonalization of the dynamical matrix that was defined within the harmonic approximation:

$$\mathbf{D}_{ij} = (m_i m_j)^{-1/2} \frac{\delta \mathbf{F}_j}{\delta \mathbf{u}_i}.$$

Here, $\mathbf{u}_i$ is the displacement vector of the appropriate atom from its equilibrium position, i and j are composite indexes that specify both atom and coordinate. m_i is the atomic mass and $\mathbf{F}_j$ is the force component in the direction of $\mathbf{u}_i$. In these calculations, the coordinates of substrate atoms were frozen and only adsorbate atoms were displaced. The force derivatives were calculated by means of a central difference approximation, with a displacement of 0.05 Å. The frequencies σ_λ were given by the eigenvalues σ_λ^2, and the normal modes by the eigenvectors $\mathbf{c}_\lambda$ of the dynamical matrix, respectively, where λ is the mode index.

The α-Al_2O_3(0 0 0 1) surface was modelled in a slab geometry, with a 2×2 repeated lateral periodicity and separated by a vacuum distance of 12 Å. Five Al_2O_3 (tri) layers were used to describe the surface, of which the two top layers were allowed to relax. The k-point sampling was preformed with a (2,2,1) Monkhorst–Pack grid [14]. Adsorption was allowed on one of the two slab surfaces, and the electrostatic potential was adjusted accordingly [15]. Three different surface terminations were considered, namely Al-terminated which is the most stable one in UHV conditions [8], hydroxyl-terminated in which the top Al atom was substituted with three hydrogen atoms placed on top of the surface oxygen atoms in each surface unit cell [7], and partially O-terminated in which one out of four top Al atoms was removed. On the different terminations, silver clusters ranging between 1 and 4 atoms were supported. The adsorption sites of α-Al_2O_3(0 0 0 1) are labeled according to common convention; i.e., the atom type immediately below the adsorption site and its corresponding surface layer determines the labeling. Ground-state structures, adsorption energies and vibrational energies of several NO_x species were calculated on all considered terminations and cluster sizes.

As reference, vibrational energies [16,17] for gas-phase NO_x are (with experimental values in parenthesis): for NO the internal vibration is 1968 (1904) cm^{-1}, while for NO_2 the asymmetric and symmetric stretch modes are 1736 (1618) and 1358 (1318) cm^{-1}, respectively. The bending mode is 717 (750) cm^{-1}. In the case of NO_3, the doubly degenerated asymmetric N–O stretch is 1291 (1492) cm^{-1}, the symmetric stretch is 1102 (1050) cm^{-1}, and finally the umbrella mode is 749 (762) cm^{-1}. Furthermore, for NO_2^- the asymmetric- and symmetric-stretch modes are 1224 and 1122 (1268, 1241) cm^{-1}, respectively. In the case of NO_3^-, the (twofold degenerated) asymmetric N–O stretches is 1366 cm^{-1} and the symmetric stretch is 1010 cm^{-1}.

3. Experimental methods

3.1. Catalyst preparation

The samples used in this study were 1 wt% Ag/α-Al_2O_3 and α-Al_2O_3. The Ag/α-Al_2O_3 sample was prepared using the method described in detail by Kylhammar et al. [18]. Briefly, the alumina powder (aluminium oxide alpha 99.99%, Johnson Matthey) was mixed with an aqueous solution of silver EDTA complexes (EDTA:$AgNO_3$ in 2.2:1 molar ratio) under continuous stirring and keeping the pH constant at 6.3. The as prepared slurry was stirred for 1 h and subsequently freeze-dried and calcined in air at 600 °C for 6 h. The α-Al_2O_3 sample was also calcined in air at 600 °C for 6 h.

3.2. In situ DRIFTS experiments

In situ FTIR (Fourier transform infrared) spectroscopy measurements were carried out using a BioRad FTS 6000 spectrometer equipped with a Harrick Praying Mantis DRIFT reaction cell [19,20]. The gases, Ar, O_2, NO and NO_2, were introduced via separate mass flow controllers (Bronkhorst Hi-Tech) to the DRIFT cell and the gas composition after the cell was probed using a quartz capillary and continuously measured by a quadrupole mass spectrometer (Balzers QMS 200).

The samples were initially pre-treated in oxygen (8% O_2 in Ar, 500 °C, 30 min) and then evacuated in pure Ar (500 °C, 15 min) at a total flow rate of 150 ml/min. Background spectra (50 scans at a resolution of 1 cm^{-1}) were collected under Ar exposure and fresh samples were used for all experiments. Adsorption of NO or NO_2 (1000 ppm in Ar) was performed at 25 °C on the α-Al_2O_3 and Ag/α-Al_2O_3 samples, respectively. The evolution of surface species during the adsorption was followed by DRIFTS for 30 min (2 scans/min at a resolution of 1 cm^{-1}).

4. Results

4.1. Theoretical characterization of the Ag–alumina system and of NO_x surface species

The Al-terminated α-Al_2O_3(0 0 0 1) is constructed by cleavage through the middle of an alumina layer in the hexagonal unit cell, thus creating a surface terminated with one single Al atom per surface unit. The OH-terminated surface is constructed by replacing the top-most Al atoms and terminating dangling bonds with H atoms (three H atoms per Al atom). To model the partially O-terminated surface, one Al atom on the (2×2) Al-terminated surface is removed. In this way, 25% of the surface is oxygen-terminated.

All three terminations of the (0 0 0 1) α-Al_2O_3 surface exhibit large surface relaxations. The results for the surface relaxations are in good agreement with previous studies [8,21]. For the hydroxyl-terminated surface, we find that one of the OH groups lie essentially parallel, whereas the other two are perpendicular to the surface plane [22]. Calculations of the vibrational properties yield O–H stretching modes with an average wavenumber of ~3720 cm^{-1}, which is in agreement with previous reports [7]. The partially O-terminated surface should be viewed as a model for a surface defect. Although the O-termination is unstable in any atmosphere, it may be allowed at the interface between Ag and Al_2O_3(0 0 0 1). Furthermore, there is a possibility that similar structure defects are frozen

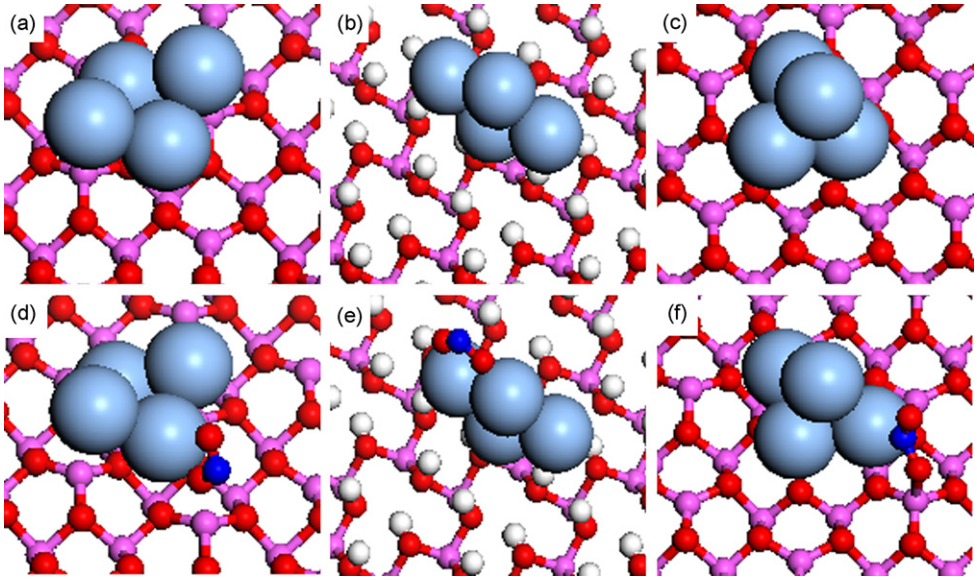

Fig. 1. Ground-state structures of Ag_4 supported on α-Al_2O_3 (top row). NO_2 adsorbed on Ag_4/α-Al_2O_3 (bottom row). The α-alumina surface terminations are: Al-terminated (left column), OH-terminated (middle column) and partially O-terminated (right column). Color code: hydrogen (white), nitrogen (blue), oxygen (red), aluminium (pink), silver (light blue). (For interpretation of the references to color in this figure legend, the reader is referred to the web version of the article.)

into the alumina matrix during the preparation of the Ag/Al_2O_3 catalysts.

The adhesion energies of Ag clusters supported on Al-terminated, OH-terminated and partially O-terminated $Al_2O_3(0\,0\,0\,1)$ surface as a function of cluster size have been reported previously [17]. In short, the calculated adhesion energy increases from 0.67 to 1.88 eV as cluster size increase from one to four Ag atoms on the Al-terminated alumina whereas on OH-terminated alumina, the adhesion energy range between 0.29 and 1.12 eV. The Ag clusters supported on the partially O-terminated surface have high adhesion energy that range between 5.5 and 6.8 eV. The results show a strong preference for Ag cluster to adsorb on the partially O-terminated $Al_2O_3(0\,0\,0\,1)$ surface. This is not surprising as the Ag cluster functions as a substitute for the missing Al atom. The relatively weak adhesion energy found on the Al-terminated and OH-terminated surfaces indicates that the Ag clusters are mobile on these surfaces.

In agreement with previous studies [21], the most favorable adsorption site for Ag_1 is above Al4 coordinating to three O ions. Ag_2 adopts a configuration that bridge Al4 and Al3 sites whereas Ag_3 forms an almost equilateral triangle, coordinating with only two atoms to the surface. Ag4 adopts a planar structure where the atoms are above 2 Al1, 1 Al3 and 1 Al4 sites (see Fig. 1a). The geometries of the supported clusters reassemble the gas-phase structures and the Ag–Ag distances are in all cases within 0.1 Å of the gas-phase counterpart [23]. On OH-terminated alumina, the ground-state structure for each cluster size is close to the corresponding gas-phase cluster and in all cases the clusters are coordinating to the surface via one single Ag atom, yielding structures perpendicular to the surface (see Fig. 1b). The strong interaction calculated for Ag clusters supported on the partially O-terminated surface is reflected in the ground-state structures. The Ag–Ag distance for Ag_2 is increased by ∼0.2 Å as compared to the gas-phase structure. For Ag_3 the smallest Ag–Ag distance increases by ∼0.1 Å and the shape changes to an equilateral triangle. A pronounced structural rearrangement is calculated for Ag_4, which forms a pyramid-like structure with an Ag–Ag distance of 2.7–2.8 Å (see Fig. 1c). In all cases, the Ag cluster moves closer to the O-terminated surface as compared to the Al- and OH-terminated surfaces. The smallest Ag–O distance range between 2.0 and 2.1 Å. The short bond distances observed indicate that Ag adsorbed on the O-terminated surface is oxidized (the Ag–O bond distance in bulk phase Ag_2O is reported experimentally to be 2.04 Å [24]).

NO, NO_2 and NO_3 adsorption are considered on all clusters and surface terminations. Considering first the bare alumina, several adsorption configurations can be envisioned. In Fig. 2a–g seven different geometries for NO_2 are shown. On the Al-terminated surface, our calculations show that the semi-bridging nitrito (Fig. 2c) is the stable configuration. Recent first-principles molecular dynamics [25] reveal that the NO_2 remains in a semi-bridging nitrito configuration at elevated temperatures, even though NO_2 occasionally can exist in a monodentate nitrito configuration (Fig. 2b). The bridging bidentate nitrito (Fig. 2d) is not possible on Al_2O_3 due to the large spatial separation (4.9 Å) between surface Al atoms. Structures a, e, f and g are not minima on the potential energy surface. The OH-terminated surface is passivated by the OH groups to that extent that none of the adsorption configurations shown in Fig. 2a–g are relevant. Instead the adsorption can be considered as a weak non-directional physisorption. As the partially O-terminated surface is unstable in any atmosphere [17], NO_2 adsorption is not considered on this termination.

For NO_3, Fig. 2h–l shows five possible adsorption configurations. Calculations show that a semi-bridging nitrato configuration is the preferred geometry (Fig. 2j). All other configurations are unstable (Fig. 2h–i and l) or not possible (Fig. 2k) for the same reason as the corresponding structure for NO_2. Recently, it was suggested [26] and later confirmed [27] that NO_x species pair up on BaO via a surface mediated electronic mechanism (Fig. 2m and n). The pairing mechanism changes the thermodynamic equilibrium in the disproportion reaction between $2NO_2 \rightarrow NO + NO_3$, with a preference for the right-hand side. The present calculations uncover that the mechanism is valid also on Al_2O_3. However, the effect is considerably smaller and amounts to 0.2 eV (Fig. 2n). For BaO the pair configuration is preferred over two NO_2 by 0.6 eV [26].

The suggested configurations in Fig. 2 are also relevant for the discussion of NO_x adsorption on supported Ag clusters. For instance, calculations show that NO_2 prefer a bridging bidentate nitrito (using one Ag atom and one Al atom) configuration on all investigated Ag clusters supported on the Al-terminated surface. Geometries where NO_2 only binds to Ag are at least 0.7 eV higher

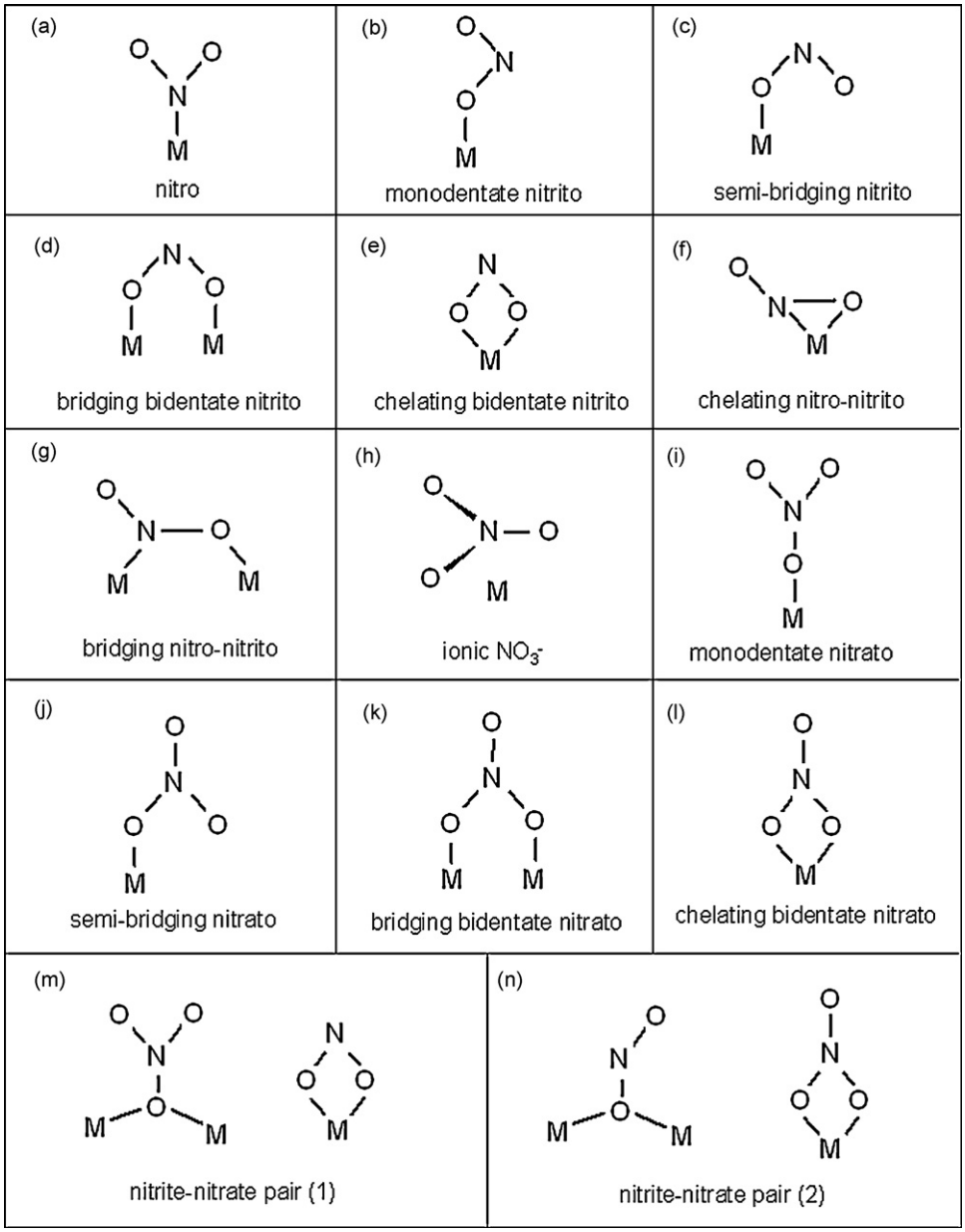

Fig. 2. Possible configurations of NO_x surface species.

in energy [17]. For the OH-terminated alumina, NO_2 is adsorbed in an atop position on the Ag_1, whereas for Ag_n, $n = 2$–4 NO_2 prefer bridge positions including only Ag atoms. This is in close analogue with adsorption geometries on gas-phase Ag clusters [23]. In the case of a partially O-terminated alumina, NO_2 prefer a nitro (Fig. 2a) configuration on the monomer. For the larger supported clusters, NO_2 favors a bridging bidentate nitrito (coordinated towards one Ag atom and one Al atom) configuration. The adsorption geometries for NO_2 on supported Ag_4 clusters are shown in Fig. 1d–f. The adsorption configuration of NO_3 follows that of NO_2, with the exception of Ag_1 supported on partially O-terminated Al_2O_3. In that case, NO_3 prefers a chelating bidantate nitrato structure.

The adsorption energy for the different NO_x species on the three considered termination of alumina is presented in Table 1. The table clearly shows that there is strong dependence on the actual termination of the α-Al_2O_3 surface. For instance, in the case of the Al-terminated surface, the adsorption energy of NO_2 range between 0.5 eV (clean) and 3.0 eV (Ag_1), whereas for the OH-terminated surface the adsorption energy range between ~0 eV (clean) and 2.2 eV (Ag_1). For both Al- and OH-terminated surfaces, the adsorption energy displays a pronounced odd-even variation as a function of cluster size. The same pattern is calculated for Ag clusters in the gas-phase [23]. In comparison the odd-even variation on partially O-terminated alumina is shifted by one cluster size.

The vibrational spectra of each NO, NO_2 and NO_3, are calculated for the three differently terminated surfaces. Most vibrational eigenvalues are below 700 cm^{-1} and belong to the surface-adsorbate vibrations. The molecular vibrational modes are presented in Table 2. The asymmetric modes are known to be dipole active, unfortunately, determination of the intensity and/or if other modes are active is not possible within the used implementation at present.

There is a clear distinction between the vibrational spectra of NO_2 species adsorbed on bare α-Al_2O_3 and on the supported Ag clusters. For instance, the wavenumber of the asymmetric mode is at least 100 cm^{-1} higher for the bare Al-terminated α-Al_2O_3 as compared to supported Ag clusters, see Table 2. For the Al- and OH-terminated surfaces, addition of Ag atoms clearly shifts the

Table 1
Calculated adsorption energies of NO, NO_2 and NO_3 on supported Ag_n clusters. The support is Al-terminated, OH-terminated and partially O-terminated α-Al_2O_3 surfaces, respectively.

	Al-terminated	OH-terminated	Partially O-terminated
NO			
Ag_0/α-Al_2O_3	−0.20	0.05	2.70
Ag_1/α-Al_2O_3	1.60	1.34	0.89
Ag_2/α-Al_2O_3	0.68	0.32	1.69
Ag_3/α-Al_2O_3	1.68	1.12	1.33
Ag_4/α-Al_2O_3	0.30	0.55	1.18
NO_2			
Ag_0/α-Al_2O_3	0.54	−0.06	–
Ag_1/α-Al_2O_3	3.05	2.20	0.86
Ag_2/α-Al_2O_3	1.70	0.79	1.95
Ag_3/α-Al_2O_3	2.80	2.07	2.37
Ag_4/α-Al_2O_3	1.84	1.34	2.15
NO_3			
Ag_0/α-Al_2O_3	1.28	0.43	1.20
Ag_1/α-Al_2O_3	3.94	2.98	1.43
Ag_2/α-Al_2O_3	2.21	1.44	2.13
Ag_3/α-Al_2O_3	3.12	2.47	2.97
Ag_4/α-Al_2O_3	2.87	2.01	1.707

asymmetric wavenumbers of adsorbed NO_2 molecules towards the corresponding wavenumbers obtained for NO_2 adsorbed on the bare Ag(1 1 1) surface (see Table 2). This effect is owing to charge transfer from the Ag clusters to the NO_2 molecule, thus forming nitrite (NO_2^-) species. Silver clusters on the partially O-terminated surface do not show the same behaviour since these species are positively charged when anchored to the partially O-terminated surface.

4.2. Experimental characterization of adsorbed NO_x surface species

The evolution of surface species during adsorption of NO and NO_2 was monitored by DRIFT spectroscopy (Figs. 3 and 4). Adsorption of NO on α-alumina results in two main adsorption features (Fig. 3a), one strong with peaks at 1630 and 1590 cm^{-1} and one weaker with peaks at 1310 and 1270 cm^{-1}. In the OH stretching region, two negative peaks at 3750 and 3720 cm^{-1} evolve with time. Simultaneously, a broad feature grows between 3700 and 3100 cm^{-1} (not shown). On the Ag/α-alumina sample, NO adsorption results in the evolution of two minor peaks at 1515 and 1235 cm^{-1} (Fig. 3b). In the OH stretching region, only a very weak negative band is observed around 3730 cm^{-1}.

Adsorption of NO_2 on α-alumina shows similar features as NO adsorption, see Fig. 4a. In addition, during the first few minutes of adsorption, a peak at 1225 cm^{-1} is visible. With time, this peak disappears or overlap with the much stronger 1260-peak. The OH stretch region shows similar peaks as for NO adsorption on α-alumina. On Ag/α-alumina (Fig. 4b), NO_2 adsorption results in a strong broad band centred around 1350 cm^{-1} and weaker peaks at 1630 and 1600 cm^{-1}, similar to the strong peaks observed for the α-alumina sample. The band centred around 1350 cm^{-1} seems to evolve from two peaks, which are formed after a few minutes of adsorption, at 1320 and 1400 cm^{-1}, respectively. During the first 5 min of adsorption, a peak develops at 1235 cm^{-1}. However, upon longer exposure this peak overlaps with other adsorption features and/or disappears. In addition, a peak is observed at 1758 cm^{-1}. In the OH stretching region only a very weak negative band evolves with time around 3730 cm^{-1}.

5. Discussion

Adsorption of NO_x surface species on various metal oxide-based materials have been widely investigated and discussed in the scientific literature, see *e.g.* [3,28]. The state and structure of NO_x surface species depend on the adsorbent material and on the reaction conditions. Infrared spectroscopy has often been used to distinguish between different types of surface species (like nitrite- and nitrate-species) as well as how the species are coordinated to the surface, *e.g.* monodentate, bidentate and bridged (see Fig. 2). The different species have all spectral features within

Table 2
Calculated wavenumbers (cm^{-1}) of the asymmetric (ν_{as1}, ν_{as2}), symmetric (ν_s), scissor (δ_s) and umbrella (ω) modes of NO, NO_2 and NO_3 on (a) supported Ag_n clusters. The support is Al-terminated, OH-terminated and partially O-terminated α-Al_2O_3 surfaces, respectively, and (b) Ag(1 1 1) surface (from [35]).

(a)	Al-terminated	OH-terminated	Partially O-terminated
α-Al_2O_3			
NO (ν)	1848	1884	–
NO_2 (ν_{as}, ν_s, δ_s)	1548, 1093, 719	1618, 1301, 710	–
NO_3 (ν_{as1}, ν_{as2}, ν_s, ω)	1506, 1292, 957, 732	1370, 1338, 1076, 768	1514, 1290, 937, 757
Ag_1/α-Al_2O_3			
NO (ν)	1649	1658	1939
NO_2 (ν_{as}, ν_s, δ_s)	1374, 1215, 771	1435, 1154, 796	1681, 1315, 756
NO_3 (ν_{as1}, ν_{as2}, ν_s, ω)	1541, 1240, 1027, 744	1574, 1240, 962, 762	1622, 1207, 988, 749
Ag_2/α-Al_2O_3			
NO (ν)	1401	1792	1856
NO_2 (ν_{as}, ν_s, δ_s)	1276, 1232, 758	1390, 1243, 764	1618, 1082, 823
NO_3 (ν_{as1}, ν_{as2}, ν_s, ω)	1576, 1237, 1051, 745	1505, 1187, 1020, 760	1498, 1277, 984, 762
Ag_3/α-Al_2O_3			
NO (ν)	1595	1591	1619
NO_2 (ν_{as}, ν_s, δ_s)	1374, 1218, 785	1289, 1260, 767	1582, 1064, 775
NO_3 (ν_{as1}, ν_{as2}, ν_s, ω)	1556, 1241, 1025, 746	1525, 1185, 1006, 752	1467, 1171, 1001, 750
Ag_4/α-Al_2O_3			
NO (ν)	1674	1780	1518
NO_2 (ν_{as}, ν_s, δ_s)	1327, 1242, 728	1347, 1236, 771	1611, 1056, 811
NO_3 (ν_{as1}, ν_{as2}, ν_s, ω)	1614, 1290, 924, 750	1566, 1167, 1015, 747	1524, 1252, 969, 744
(b)	Ag(1 1 1) (cm^{-1})		
NO (ν)	1647		
NO_2 (ν_{as}, ν_s, δ_s)	1371, 1226, 762		
NO_3 (ν_{as1}, ν_{as2}, ν_s, ω)	1608, 1159, 973, 752		

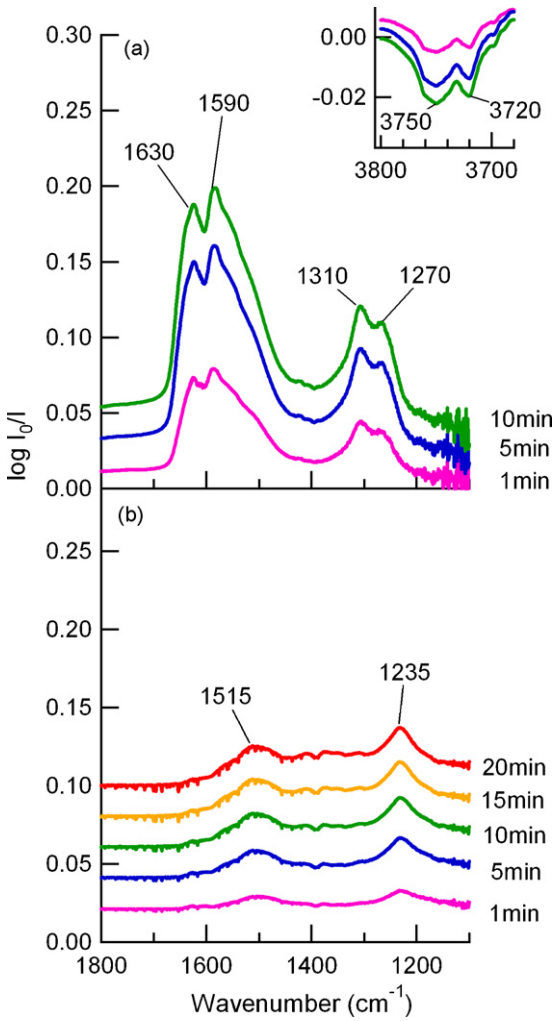

Fig. 3. Evolution of surface species during NO adsorption at 25 °C over (a) α-alumina and (b) Ag/α-alumina.

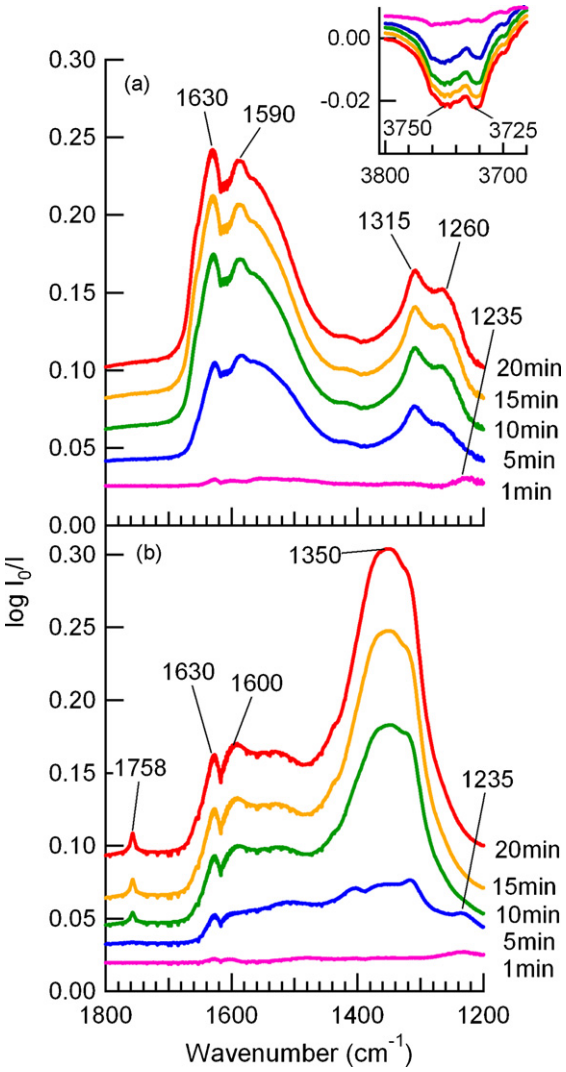

Fig. 4. Evolution of surface species during NO_2 adsorption at 25 °C over (a) α-alumina and (b) Ag/α-alumina.

a narrow region (1800–1100 cm^{-1}), which gives rise to overlapping bands and obstructs exact assignment. However, using first-principles calculations of vibrational frequencies for different NO_x surface species may provide the possibility of identification.

In this work, the main NO_x related features observed over α-alumina are two broad features with strong peaks at 1630 and 1590 cm^{-1} and weaker peaks at 1310 and 1270 cm^{-1}. On the Ag/α-alumina sample, NO_2 adsorption gives rise to a strong broad band centred around 1350 cm^{-1}, and a broad feature with peaks at 1630 and 1600 cm^{-1}. In the literature, bands in the spectral regions 1650–1500 and 1300–1170 cm^{-1} have generally been assigned to the asymmetric stretch vibrations of nitrates on metal oxides *e.g.* [29,30]. However, the large amount of vibrational modes (Table 3) in this frequency range stresses the difficulty of assignment. Nevertheless, the literature data suggests that surface species found in the present experiments are combinations of surface nitrite- and nitrate-species and/or adsorbed NO_2 species.

In Table 2, the calculated vibrational modes of NO, NO_2 and NO_3 on α-alumina and Ag_n (n = 1–4) clusters supported on α-alumina are shown. When the calculated values are compared with the experimental results it is evident that the surface species are combinations of nitrite- and nitrate-species and, in some cases, also adsorbed NO_2. For comparison, the calculated vibrational modes for NO, NO_2 and NO_3 on Ag(1 1 1) surface are shown in Table 2. As the particles in the present study are large (likely >5 nm), these values are applicable for the interpretation of the experimental results.

In Figs. 5 and 6, the vibrational modes for NO_2 and NO_3 on α-alumina and supported Ag_n (n = 1–4) clusters are visualised and compared to the experimental spectra. It is clearly seen, that the cluster size and the surface termination influence the peak positions. Comparison with the broad features in the experimental spectra gives reason to assume several types of NO_x surface species on different types of sites. Thus, it is likely that the powder Ag/α-alumina sample contains a variety of metal sites as well as different surface terminations that result in several, sometimes overlapping, peaks. In this sense, the spectra obtained from the DRIFTS experiments are mean-values. Due to the overlapping bands, the peaks in the resulting spectra are difficult to assign unambiguously. Instead these spectral features may be associated with combinations of several types of species, such as NO, NO_2 and NO_3. This also implies that it is not straightforward to ascribe peaks to specific adsorption configurations.

However, by the use of previous assignments together with calculated wavenumbers in the present work, some conclusions regarding surface species are possible. The spectral features in the 1650–1200 cm^{-1} range can be assigned to a combination of nitrite- and nitrate-surface species as well as adsorbed NO_2. Over the Ag-free α-Al_2O_3, the broad feature at 1680–1460 cm^{-1} may be

Table 3
Literature assignments of NO_x surface species. The table refers to representative sources.

NO_x surface specie	Wavenumber (cm^{-1})	System	Ref.
Adsorbed NO_x species	1560	Ag/Al_2O_3, Al_2O_3	[36,37]
Adsorbed NO_2 species	1615	Ag/Al_2O_3	[38]
Monodentate nitrite (NO_2^-)	1470–1450	Me/oxide	[3]
Nitro (NO_2^-)	1440–1335	Me/oxide	[3]
Chelating nitro-nitrito (NO_2^-)	1520–1390	Me/oxide	[3]
Bridging bidentate	1220–1205	Me/oxide	[3]
nitrite (NO_2^-)	1230	Ag/Al_2O_3	[37]
Nitrite (NO_2^-)	1235	Ag/Al_2O_3, Al_2O_3	[36]
Adsorbed N_2O_4	1758–1730, 1359–1368	Me/oxide	[3]
Monodentate nitrate	1530–1480, 1290–1250	Me/oxide	[3]
(NO_3^-)	1558, 1297	Ag/Al_2O_3	[38]
	1550, 1245	Ag/Al_2O_3	[37]
Bidentate nitrate	1565–1500, 1300–1260	Me/oxide	[3]
(NO_3^-)	1586, 1248	Ag/Al_2O_3	[38]
	1590, 1295	Ag/Al_2O_3	[37]
Bridging nitrate (NO_3^-)	1650–1600, 1225–1170	Me/oxide	[3]
	1615	Ag/Al_2O_3	[29]
Nitrate (NO_3^-)	1550, 1250	Ag/Al_2O_3, Al_2O_3	[36]
	1590, 1305		
Ionic NO_3^-	1380	Me/oxide	[3]

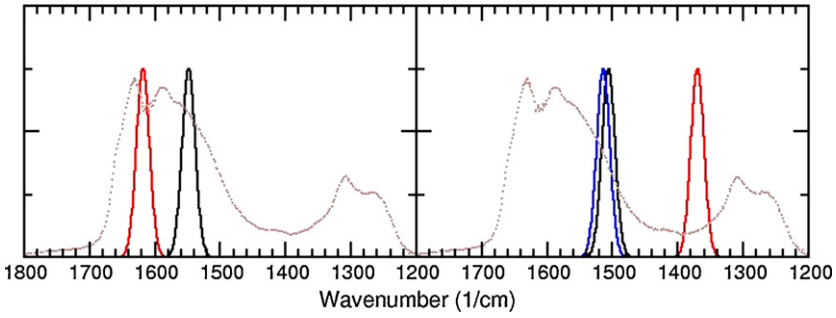

Fig. 5. Vibrational spectra of NO_2 adsorption at 25 °C on α-alumina, obtained from measurements (grey dotted line), and theoretical calculations of NO_2 (left-hand side) and NO_3 (right-hand side) species on the surface. The calculations are furthermore separated according to the actual surface termination, Al- (black), OH- (red) and partially O- (blue), respectively. (For interpretation of the references to color in this figure legend, the reader is referred to the web version of the article.)

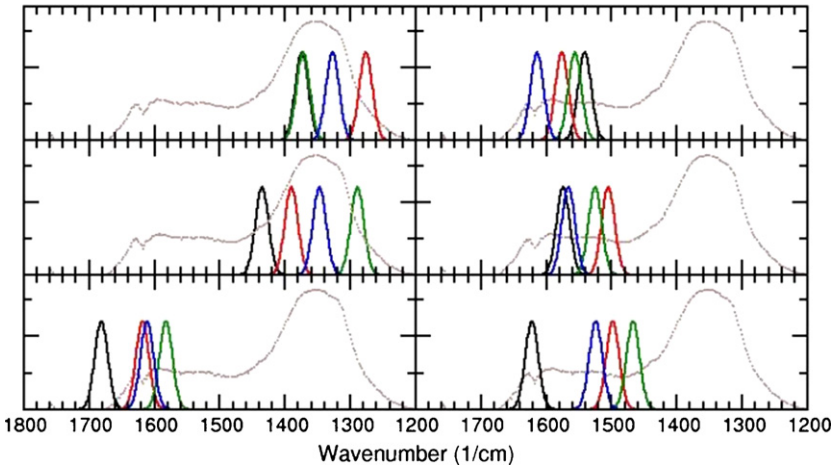

Fig. 6. Vibrational spectra of NO_2 adsorption at 25 °C on Ag/α-alumina, obtained from measurements (grey dotted line), and theoretical calculations of NO_2 (left-hand column) and NO_3 (right-hand column) species on the surface. The calculations are furthermore separated according to the actual surface termination, Al- (upper row), OH- (middle row) and partially O- (bottom row), respectively. The color code refers to the Ag cluster size, Ag_1 (black), Ag_2 (red), Ag_3 (green) and Ag_4 (blue). (For interpretation of the references to color in this figure legend, the reader is referred to the web version of the article.)

assigned to surface nitrate (NO_3^-) species and/or loosely bound NO_2 (see Tables 2 and 3 and Fig. 5). Nitrite (NO_2^-) species are not likely to form directly over the Ag-free alumina sample as the charge transfer from alumina to NO_2 is not complete (0.57 electrons).

Experimentally, a broad band is formed between 1440 and 1260 cm^{-1} during NO_2 adsorption over Ag/α-Al_2O_3. This corresponds to nitrite species (see Tables 2 and 3 and Fig. 6). Over the Ag/α-Al_2O_3 sample, especially in the case of Al- and OH-terminated surfaces, nitrites are likely to form owing to charge transfer from the silver cluster to the NO_2 molecule. The charge transfer is calculated to be 0.84, 0.62 and 0.24 electrons for the Al-, OH- and partially O-terminated surfaces, respectively. Furthermore, using the results from the calculations, peaks in the area 1630–1590 cm^{-1} can be assigned to loosely bound NO_2 and the broad band(s) at 1600–1460 cm^{-1} can be attributed to nitrate surface species (Fig. 6). The peak at 1758 cm^{-1} has been ascribed to the asymmetric stretching of NO_2 originating from N_2O_4 [3,29,31,32]. This is not likely as the peak is not present for the Ag-free sample. Alternatively, this peak may be attributed to a combinational mode for NO_3 stretching vibrations of ionic nitrate [33]. In the OH stretching region, the peaks at 3750 and 3720 cm^{-1} and the broad feature between 3700 and 3100 cm^{-1} are assigned to OH groups on the alumina surface and to perturbed OH stretching vibrations, respectively [34].

6. Conclusion

In this work, the adsorption of NO_x species on α-alumina and Ag/α-alumina has been investigated by *in situ* DRIFT spectroscopy and DFT calculations. The measured IR spectra show broad features that can be assigned to different NO_x surface species. This is a manifestation of the heterogeneous nature of the samples, including different surface terminations and adsorption sites. As a consequence, exact assignments of specific surface species, especially with specific configurations on the surface, are difficult to obtain. The results from the calculations show that different sizes of the silver clusters and different surface terminations on α-alumina strongly influence the positions of the vibrational modes. In this sense, first-principles calculations can guide the assignment of NO_x surface species.

Acknowledgements

This work is financially supported by MISTRA (The Foundation for Strategic Environmental Research), and has been performed as part of the E4 programme (Energy Efficient Reduction of Exhaust Emissions from Vehicles). The work has been performed at the Competence Centre for Catalysis, which is financially supported by Chalmers University of Technology, the Swedish Energy Agency and the member companies: AB Volvo, Volvo Car Corporation, Scania CV AB, GM Powertrain Sweden AB, Haldor Topsø A/S and The Swedish Space Corporation.

References

[1] R. Burch, Catal. Rev. Sci. Eng. 46 (2004) 271.
[2] K. Shimizu, A. Satsuma, Phys. Chem. Chem. Phys. 8 (2006) 2677–2695.
[3] K.I. Hadjiivanov, Catal. Rev. Sci. Eng. 42 (2000) 71.
[4] P. Broqvist, H. Grönbeck, E. Fridell, I. Panas, Catal. Today 96 (2004) 71.
[5] P. Broqvist, H. Grönbeck, E. Fridell, I. Panas, J. Phys. Chem. B 108 (2004) 3523.
[6] A. Desikusumastuti, T. Staudt, H. Grönbeck, J. Libuda, J. Catal. 255 (2008) 127.
[7] K.C. Hass, W.F. Schneider, A. Curioni, W. Andreoni, Science 282 (1998) 265.
[8] X.G. Wang, A. Chaka, M. Scheffler, Phys. Rev. Lett. 84 (2000) 3650.
[9] J.M. McHale, A. Auroux, A.J. Perrotta, A. Navrotsky, Science 277 (1997) 788.
[10] S.R. Bahn, K.W. Jacobsen, Comput. Sci. Eng. 4 (2002) 56.
[11] B. Hammer, L.B. Hansen, J.K. Norskov, Phys. Rev. B 59 (1999) 7413.
[12] D. Vanderbilt, Phys. Rev. B 41 (1990) 7892.
[13] J.P. Perdew, K. Burke, M. Ernzerhof, Phys. Rev. Lett. 78 (1997) 1396.
[14] H.J. Monkhorst, J.D. Pack, Phys. Rev. B 13 (1976) 5188.
[15] L. Bengtsson, Phys. Rev. B 59 (1999) 12301.
[16] R.D. Johnson, NIST Computational Chemistry Comparison and Benchmark Database, NIST Standard Reference Database Number 101, Release 12, 2005 (http://srdata.nist.gov/cccbdb).
[17] A. Hellman, H. Grönbeck, J. Phys. Chem. C 113 (9) (2009) 3674.
[18] L. Kylhammar, A. Palmqvist, M. Skoglundh, Top. Catal. 42–43 (2007) 119.
[19] H.H. Ingelsten, A. Palmqvist, M. Skoglundh, J. Phys. Chem. B 110 (2006) 18392.
[20] R. Matarrese, H.H. Ingelsten, M. Skoglundh, J. Catal. 258 (2008) 386.
[21] R. Meyer, Q.F. Ge, J. Lockemeyer, R. Yeates, M. Lemanski, D. Reinalda, M. Neurock, Surf. Sci. 601 (2007) 134.
[22] Z. Lodziana, J.K. Norskov, P. Stoltze, J. Chem. Phys. 118 (2003) 11179.
[23] H. Grönbeck, A. Hellman, A. Gavrin, J. Phys. Chem. A 111 (2007) 6062.
[24] R.W.G. Wyckoff, Crystal Structures, vol. II, John Wiley & Sons, New York, 1963.
[25] A. Hellman, H. Grönbeck, Phys. Rev. Lett. 100 (2008) 116801.
[26] P. Broqvist, I. Panas, E. Fridell, H. Persson, J. Phys. Chem. B 106 (2002) 137.
[27] C.W. Yi, J.H. Kwak, J. Szanyi, J. Phys. Chem. C 111 (2007) 15299.
[28] M.A. Hitchman, G.L. Rowbottom, Coord. Chem. Rev. 42 (1982) 55.
[29] S. Kameoka, Y. Ukisu, T. Miyadera, Phys. Chem. Chem. Phys. 2 (2000) 367.
[30] K. Shimizu, H. Kawabata, A. Satsuma, T. Hattori, J. Phys. Chem. B 103 (1999) 5240.
[31] Q. Sun, Z.X. Gao, B. Wen, W.M.H. Sachtler, Catal. Lett. 78 (2002) 1.
[32] J. Szanyi, M.T. Paffett, J. Catal. 164 (1996) 232.
[33] A. Desikusumastuti, M. Happel, K. Dumbuya, T. Staudt, M. Laurin, J.M. Gottfried, H.P. Steinruck, J. Libuda, J. Phys. Chem. C 112 (2008) 6477.
[34] G. Busca, Phys. Chem. Chem. Phys. 1 (1999) 723.
[35] A. Hellman, I. Panas, H. Grönbeck, J. Chem. Phys. 128 (2008) 104704.
[36] F.C. Meunier, J.P. Breen, V. Zuzaniuk, M. Olsson, J.R.H. Ross, J. Catal. 187 (1999) 493.
[37] P. Sazama, L. Capek, H. Drobna, Z. Sobalik, J. Dedecek, K. Arve, B. Wichterlova, J. Catal. 232 (2005) 302.
[38] J. Shibata, K. Shimizu, S. Satokawa, A. Satsuma, T. Hattori, Phys. Chem. Chem. Phys. 5 (2003) 2154.